

# Large-scale Motions in the Universe: Observations and Simulations

D. H. Gudehus

*Physics and Astronomy Department, Georgia State University, Atlanta, GA 30303*

**Abstract.** The peculiar radial velocities of eight clusters of galaxies, as determined from a variety of distance indicators, are consistent with a bulk flow not greatly different in direction and magnitude from the velocity vector of the Local Group relative to the microwave background radiation. The bulk flow vector is directed to  $l = 266^\circ \pm 18^\circ, b = 17^\circ \pm 15^\circ$  with a magnitude of  $788 \pm 113 \text{ km s}^{-1}$ . N-body simulations of gravitationally induced peculiar motions from a set of over 1000 clusters of known redshift give reasonably good agreement for the peculiar velocities of the Local Group and Virgo both in magnitude and direction. Most of the accelerating mass lies within about  $40h^{-1}$  Mpc but more distant clusters are necessary to fully account for the magnitude and direction.

## 1. Introduction

It has been more than 25 years since the first peculiar velocity of a cluster of galaxies was reported (Gudehus 1973), more than 20 years since peculiar velocities were first referenced to the microwave background radiation (MBR) (Gudehus 1978), accurately measured for the first time by Smoot, Gorenstein, and Muller (1977), and more than 10 years since Dressler *et al.* (1987) first reported that galaxian peculiar velocities were correlated in direction. The first part of this time period, however, was marked by the fixed idea that the universal expansion was “quiet” (Visvanathan and Sandage 1977 and references therein; Tammann 1984). Tammann (1984), for example, claimed that my 1978 peculiar velocity for Virgo was “impossible in size *and* sign”. These early contrary claims have been explained (Gudehus 1989b, 1991) as due to *i*) a neglect to reference redshifts to the MBR frame and *ii*) a variety of systematic effects. The current view is that peculiar velocities exist at some level out to  $15,000 \text{ km s}^{-1}$ , but with some observers finding significantly smaller values at greater distance (Riess *et al.* 1995; Giovanelli *et al.* 1998) than others (Gudehus 1989b; Lucey *et al.* 1991; Bothun *et al.* 1992; Mould *et al.* 1993; Hudson *et al.* 1999); Willick (1999), and one group (Lauer & Postman 1994) finding a significantly different vector direction for the most distant clusters.

In this paper I will use relative distance moduli taken from my previous studies, solve for a preferred set of revised cluster peculiar velocities, and compute an average direction for the cosmic flow. I will then, from an N-body

simulation based on masses assigned to clusters of known redshift, calculate predicted peculiar velocities for the LG and Virgo.

## 2. The Data

The data sets used in this study comprise  $m^*$  magnitudes (Gudehus 1989b) for ten clusters, reduced galaxian radius parameters,  $r_g$ , (Gudehus 1991) for four clusters, and relative magnitudes of seventeen selected clusters computed as weighted averages from several independent distance indicators (Gudehus 1995) (including first-ranked magnitude and richness-corrected nuclear magnitudes). The  $m^*$  and  $r_g$  data were combined and fitted by nonlinear least squares to the redshift-magnitude diagram with  $q_0$  assumed to be 0.5, luminosity evolution assumed to be 0.75 magnitudes per unit  $z$ , and all redshifts corrected to the Cosmic Background Explorer (COBE) results for the LG's motion relative to the MBR (Smoot *et al.* 1991). The nearest five clusters were given zero weight in the fit since their peculiar velocities produce substantial deviations from the curve and are nonrandomly distributed. The standard deviation about the curve fitted to the remaining points is 0.064 mag. Peculiar velocities were derived from the selected clusters in a similar way and include three duplicates from the first set, i.e., Virgo, Fornax, and Hydra I, which were given zero weight in the fit. Although the standard deviation about the fit is larger, i.e., 0.11 mag, than for the first set, the preferred peculiar velocities of the duplicates are taken from the second set since in that set each cluster's point represents a weighted average of several independent distance indicators (three for Fornax and Hydra I, and six for Virgo). Table 1 lists for each cluster, the peculiar velocity observations. Column 1 gives the identity, column 2 the redshift velocity relative to the MBR, column 3 the distance modulus relative to Virgo consistent with the peculiar velocities, and column 4 the radial peculiar velocity, respectively.

Table 1. Cluster Peculiar Velocity Data.

Cluster	$cz_u$ ( $\text{km s}^{-1}$ )	$\Delta m$	$v_{r,\text{pec}}$ ( $\text{km s}^{-1}$ )
Virgo	1473	0.00	$387 \pm 66$
Ursa Major	1140	0.25	$-79 \pm 111$
Fornax	1428	0.26	$202 \pm 78$
Hydra I	4027	2.44	$665 \pm 167$
Perseus	5179	3.62	$-541 \pm 399$
A1367	6880	3.71	$883 \pm 200$
Coma	7185	4.06	$165 \pm 214$
A2199	9081	4.71	$-335 \pm 297$

Figure 1 shows the radial peculiar velocity vectors projected on the best fitting plane passing through the eight clusters. The pole of this plane is in the direction  $\alpha = 6^{\text{h}}7$ ,  $\delta = 16^\circ$ , or  $l = 198^\circ$ ,  $b = 6^\circ$  (1950.0 equinox). The angle between the pole and the MBR apex is  $77^\circ$ . The angle between the pole and the supergalactic pole is  $31^\circ$ .

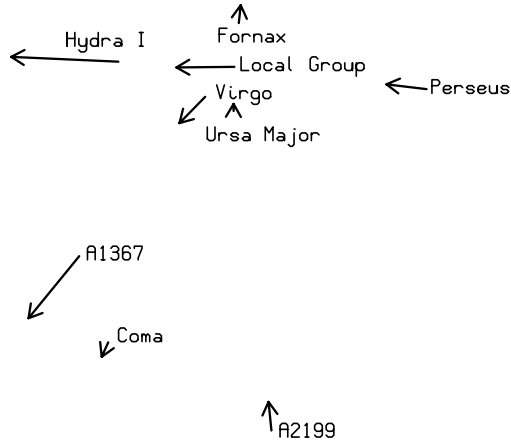


Figure 1. Peculiar radial velocity vectors of eight nearby clusters as projected on the best-fitting plane through their positions on the sky. The weighted average of the vectors, excluding the Local Group, is directed towards  $l = 272^\circ \pm 18^\circ$ ,  $b = 48^\circ \pm 15^\circ$ , and differs by  $19^\circ$  from the direction of the Local Group's motion relative to the MBR.

A bulk flow vector, solved for by nonlinear least squares, is directed to  $l = 266^\circ \pm 18^\circ$ ,  $b = 17^\circ \pm 15^\circ$  with a magnitude of  $788 \pm 113 \text{ km s}^{-1}$ . The mean error of the fit is  $136 \text{ km s}^{-1}$ , and the vector differs by  $15^\circ$  from the direction of the LG's motion relative to the MBR. The average depth is  $4549 \text{ km s}^{-1}$  and the average weighted depth is  $2214 \text{ km s}^{-1}$ . Bulk flow tangential velocity components added to the observed radial components give the space vectors plotted in Figure 2. In Figure 3 I have plotted on a Hammer-Aitoff projection in galactic coordinates, the directions of the bulk flow vectors of this study and several others.

### 3. Simulations

In the simulations presented here I consider the gravitational accelerations due to clusters of galaxies for which redshifts are presently known. In the first step of the simulation calculation, clusters within a given redshift range are selected from a catalogue of all known clusters. For each cluster the coordinates and distances based on a given Hubble parameter,  $H_0$  and deceleration parameter,  $q_0$ , are computed. The distances are then reduced to values appropriate for a young universe and the model universe allowed to expand. At each uniform time step, the acceleration from each cluster on the LG and Virgo are computed, and the velocities are computed from the integrals. Ten free parameters are used in the simulation. Besides  $H_0$  and  $q_0$ , there are the mass of a richness 2 cluster,  $\mathcal{M}_2$ ; the factor to be applied to the number of galaxies in a richness 0 cluster in describing a cluster of unknown richness,  $F$ ; the power describing how cluster mass scales with richness (see below),  $P$ ; the age of the universe at the beginning of the calculation,  $t_1$ ; the minimum distance allowed between clusters,  $r_{\min}$ ; the

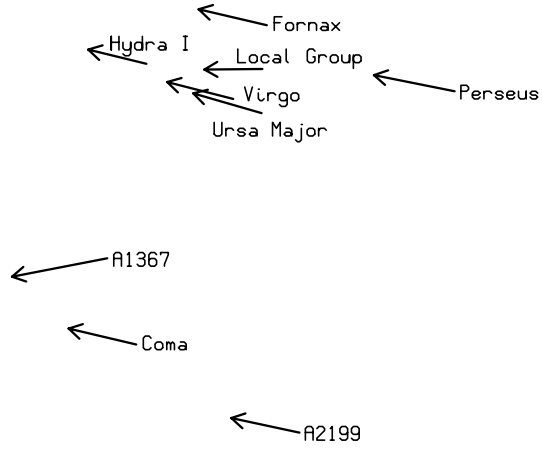


Figure 2. Peculiar space velocity vectors of eight nearby clusters as projected on the best-fitting plane through their positions on the sky. The tangential components are taken from a bulk velocity vector fitted to the radial components by nonlinear least squares. The bulk flow vector is directed towards  $l = 266^\circ \pm 18^\circ$ ,  $b = 17^\circ \pm 15^\circ$  with a magnitude of  $788 \pm 113 \text{ km s}^{-1}$ , and differs by  $15^\circ$  from the direction of the Local Group's motion relative to the MBR.

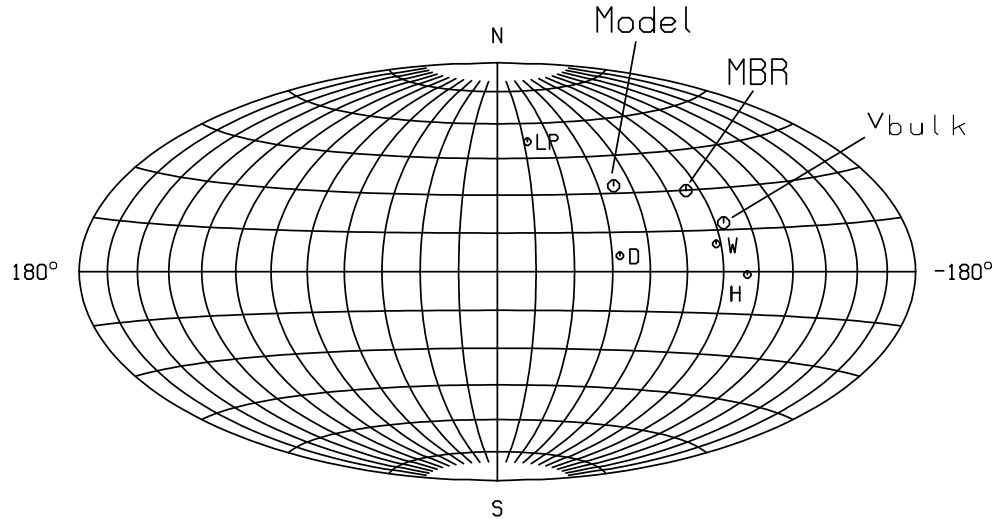


Figure 3. The directions, on a Hammer-Aitoff projection in galactic coordinates, of the observed bulk flow velocity vectors of the present study and those of Dressler *et al.* (1987) (D), Hudson *et al.* (1999) (H), Lauer and Postman (1994) (LP), and Willick (1999) (W), all with respect to the microwave background radiation (MBR), whose direction is shown as well. Also shown is the direction of the LG's motion as derived from an N-body simulation with 1009 clusters of known redshift.

number of time steps,  $N$ ; and the minimum and maximum redshifts used in selecting the clusters from the catalogue,  $z_{\min}$  and  $z_{\max}$ .

The cluster mass,  $\mathcal{M}_2$ , was taken from Abell (1974) and Kent and Gunn (1982) as  $2.3 \times 10^{15} \mathcal{M}_{\odot}$ , and  $F$  was arbitrarily set at 0.1. Richer clusters contain a proportionally greater amount of light which exceeds the ratio of increase in the number of their member galaxies, because the luminosity functions of richer clusters extend to brighter magnitudes (Gudehus 1995). The amount of mass in richer clusters increases faster than the rate of luminosity increase because richer clusters possess higher mass-to-luminosity ratios (Davies, *et al.* 1980). I model cluster mass as a function of number of galaxies of a given richness by the relation  $\mathcal{M}_r = \mathcal{M}_2(n_r/n_2)^P$ , where  $n$  is the average number in a richness class. An estimate of  $P$  can be obtained from the velocity dispersions in clusters of two different richnesses. Taking values for the Coma cluster (Kent and Gunn 1982) and cluster A1689 (Gudehus 1989a), I derive  $P = 2.1$ . Based on Larson (1969), the age at the beginning of the calculation is taken to be  $1.0 \times 10^9$  y. The minimum cluster separation is assumed to be 1 Mpc, but this parameter rarely comes into play. The Hubble constant is taken to be  $70 \text{ km s}^{-1} \text{ Mpc}^{-1}$ . A number of time steps equal to 1000 gives sufficient accuracy, and the redshift limits are taken as 0 and 0.3.

A simulation with the above values includes 1009 clusters of which 1 is of richness 5, 10 of richness 4, 61 of richness 3, 131 of richness 2, 257 of richness 1, 358 of richness 0, and 190 of unknown richness. The resultant peculiar velocities and galactic coordinates of the vectors are shown in Table 2. Increasing  $P$  to 2.8 gives better agreement with the observed velocities of the LG and Virgo's radial peculiar velocity. The angular deviation of the LG's direction from the MBR is  $27^\circ$ . The direction for the simulation with  $P = 2.8$  has been included in Figure 3.

Table 2. Cluster Peculiar Velocity Simulations.

$P$	$v_{\text{LG}}$ ( $\text{km s}^{-1}$ )	$v_{\text{Virgo}}$ ( $\text{km s}^{-1}$ )	$v_{r,\text{Virgo}}$ ( $\text{km s}^{-1}$ )	long <sub>LG</sub> long <sub>Virgo</sub>	lat <sub>LG</sub> lat <sub>Virgo</sub>
2.1	600	584	162	$304^\circ$ $316^\circ$	$23^\circ$ $3^\circ$
2.8	626	712	348	$308^\circ$ $317^\circ$	$33^\circ$ $17^\circ$

Figure 4 shows a smoothed false color plot of the mass assigned to the clusters closer than  $z = 0.07$  and which lie within  $45^\circ$  of the best-fitting plane through the eight nearby clusters. Since the best fitting  $P$  is greater than the value based on known cluster masses, i.e., 2.1, increasing amounts of mass are contained outside the richer clusters. Figure 5 shows how the model velocity for the LG depends on upper redshift limit. Most of the accelerating masses lie within about  $40h^{-1}$  Mpc ( $z = 0.013$ ), but more distant clusters, such as those at  $150h^{-1}$  Mpc ( $z = 0.05$ ) contribute as well. Convergence to a steady value occurs only after a distance of about  $450h^{-1}$  Mpc ( $z = 0.15$ ) is reached.

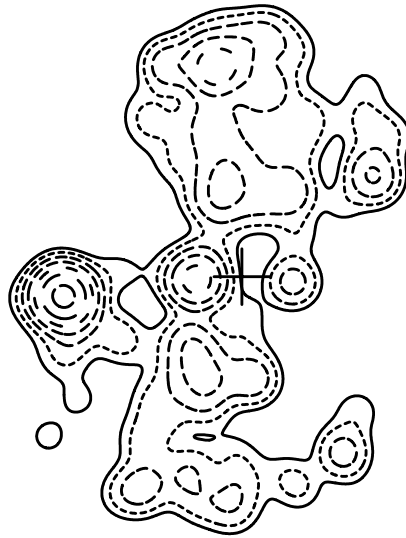


Figure 4. A contour plot of mass in the N-body model used for simulating peculiar motions, which is associated with clusters of known redshift that are closer than  $z = 0.07$ , and which lie within 45 degrees of the best-fitting plane through the eight nearby clusters. The locations, representing 366 clusters, were smoothed with a gaussian of  $1232 \text{ km s}^{-1}$ . The Local Group is at the center. The peaks represent extragalactic mass concentrations (EMACS) made up of very rich clusters and their associated dark matter. For example, the peak at the left at about  $z = 0.05$  includes the richness 4 cluster Abell 3558 and the richness 3 cluster Abell 3559. The Perseus cluster is the small peak just to the right of center. The MBR flow is to the left.

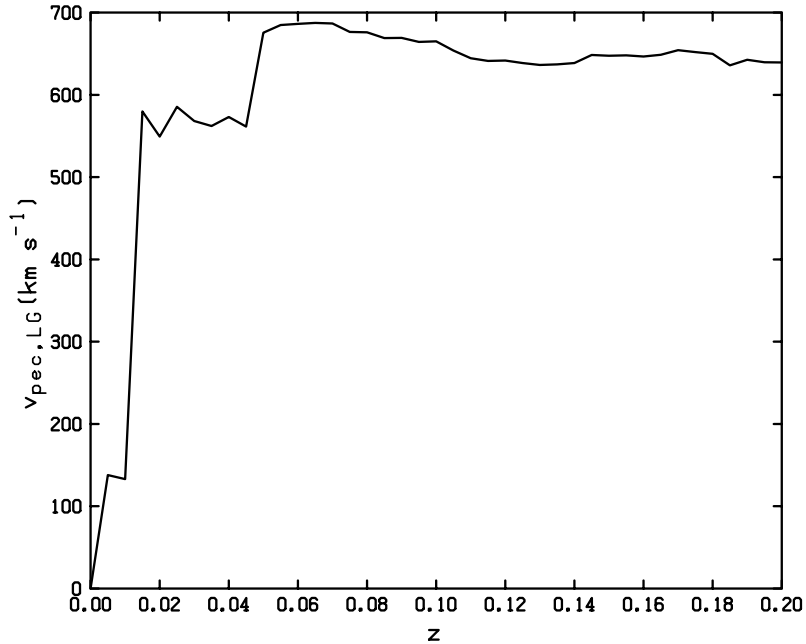


Figure 5. The magnitude of the peculiar velocity of the Local Group as a function of the upper redshift limit of the N-body model. Most of the peculiar velocity is accounted for by clusters within about  $40 h^{-1}\text{Mpc}$  ( $z = 0.013$ ). An additional contribution at  $150 h^{-1}\text{Mpc}$  ( $z = 0.05$ ) arises from clusters which include Abell 3558 and Abell 3559. Convergence to a steady value is reached after about  $450 h^{-1}\text{Mpc}$  ( $z = 0.15$ ).

#### 4. Summary

Both the magnitude and direction of the observed average radial peculiar velocity are consistent with the set of eight clusters participating in the same flow that the LG moves with. Gudehus's (1995) observation that when the measured infall to Virgo of  $52 \text{ km s}^{-1}$  is used to compute the LG's undisturbed velocity vector, the projected radial velocity precisely matches Virgo's measured radial peculiar velocity, demonstrates that at least Virgo participates in the flow. Other clusters in that study also showed evidence of flow participation.

Simulations for gravitationally induced peculiar motions in an expanding universe with model parameters set equal to reasonable values drawn from the literature give acceptable agreement with the observed velocities of the LG and Virgo. The sparseness of the cluster catalogue prevents extending the calculation to more distant clusters at this time.

#### References

- Abell, G. 1974 in *Galaxies and the Universe*, Vol. IX of *Stars and Stellar Systems*, Sandage, A., Sandage, M. & Kristian, J., Chicago: Univ. of Chicago Press, 601

- Aaronson, M., Bothun, G. D., Cornell, M. E., Dawe, J. A., Dickens, R. J., Hall, P. J., Sheng, H. M., Huchra, J. P., Lucey, J. R., Mould, J. R., Murray, J. D., Schommer, R. A., & Wright, A. E. 1989, *ApJ*, 338, 654
- Bothun, G. D., Schommer, R. A., Williams, T. B., Mould, J. R., & Huchra, J. P. 1992, *ApJ*, 388, 253
- Davis, M., Tonry, J., Huchra, J. & Latham, D. 1980 *ApJ*, 238, L113
- Dressler, A., Faber, S., Burstein, D., Davies, R., Lynden-Bell, D., Terlevich, R. J., & Wegner, G. 1987, *ApJ*, 313, L37
- Giovanelli, R., Haynes, M., Salzer, J., Wegner, G., Da Costa, L., & Freudling, W. 1998, *AJ*, 116, 2632
- Gudehus, D. H. 1973, *AJ*, 78, 583
- Gudehus, D. H. 1978, *Nature*, 275, 514
- Gudehus, D. H. 1989a, *ApJ*, 340, 661
- Gudehus, D. H. 1989b, *ApJ*, 342, 617
- Gudehus, D. H. 1991, *ApJ*, 382, 1
- Gudehus, D. H. 1995, *A&A*, 302, 21
- Hudson, M. J, Smith, R. J., Lucey, R. R., Schlegel, D. J. & Davies, R. L. 1999, *ApJ*, 512, L79
- Kent, S. & Gunn, J. 1982, *AJ*, 87, 945
- Larson, R. 1969, *MNRAS*, 145, 405
- Lucey, J. R., Gray, P. M., Carter, D., & Terlevich, R. J. 1991, *MNRAS*, 248, 804
- Mould, J. R., Akeson, R. L., Bothun, G. D., Han, M., Huchra, J. P., Roth, J. & Schommer, R. A. 1993, *ApJ*, 409, 14
- Riess, A., Press, W., & Kirshner, R. 1995, *ApJ*, 445, L91
- Smoot, G. F., Gorenstein, M. V., & Muller, R. A. 1977, *Phys.Rev.Lett*, 39, 898
- Smoot, G. et al. 1991, *ApJ*, 371, L1
- Tammann, G. A. 1984, in *Clusters and Groups of Galaxies*, F. Mardirossian *et al.* Dordrecht: Reidel 529
- Visvanathan, N. & Sandage, A. R. 1977, *ApJ*, 216, 214
- Willick, J. 1999, *ApJ*, (in press)